13th Australasian Fluid Mechanics Conference
Monash University, Melbourne, Australia
13-18 December 1998

DYNAMICS OF THE VELOCITY GRADIENT TENSOR IN TURBULENT BOUNDARY LAYER FLOW

C. J. BULBECK[1], M.S. CHONG[2] and J. SORIA[3]
[1]AMRL, DSTO, Fishermens Bend, Victoria 3207, AUSTRALIA
[2]Dept. Mech. & Man. Eng., University of Melbourne, Parkville, Victoria 3052, AUSTRALIA
[3]Dept. Mech. Eng., Monash University, Clayton, Victoria 3168, AUSTRALIA

ABSTRACT

Using Direct Numerical Simulation (DNS) of the Navier-Stokes equations for incompressible turbulent boundary layer flow, Conditional Mean Trajectories (CMTs) of invariants of the velocity gradient, rate-of-strain and rate-of-rotation tensors are computed and compared with solution trajectories of modelled equations for the evolution of the velocity gradient tensor.

INTRODUCTION

Investigations of the invariants of the velocity gradient tensor have proven useful in analysing the fine-scale structure of turbulent fluid flow. By differentiating the Navier-Stokes equations with respect to the three spatial co-ordinates, an equation for the evolution of the velocity gradient tensor can be derived. Several simplifying assumptions have been proposed in the analysis of this equation. Vieillefosse (1984) and Cantwell (1992) studied the case in which the anisotropic pressure and viscous terms in the equation were neglected giving the restricted Euler equation. Vieillefosse (1984) found that the solution of the restricted Euler equation evolved to a state where the vorticity vector is aligned with the eigenvector corresponding to the intermediate rate-of-strain, and where the intermediate rate-of-strain is positive. Cantwell (1992) solved the restricted Euler equation analytically, and found that although the solution diverges in finite time, it also evolves along lines of constant discriminant. Martín & Dopazo (1995) proposed a model for the viscous terms of the evolution equation for the velocity gradient tensor, while still neglecting the anisotropic pressure terms, and found that the solution converged for certain initial conditions, an improvement over the restricted Euler model. Recently Martin *et al.* (1997) used data from a DNS of homogeneous isotropic turbulence to make a detailed study of the evolution of the velocity gradient tensor. They were able to use the concept of Conditional Mean Trajectories (CMTs) of the invariants of the velocity gradient tensor in phase space to compare their DNS results with the models, and found the models somewhat lacking in being able to reproduce significant features of the flow.

The evolution of the velocity gradient tensor in turbulent boundary layer flow will be examined in this paper. The CMTs of invariants in the turbulent boundary layer will be compared with the various models.

NUMERICAL EXPERIMENT

The numerical method for DNS of the boundary layer is described in detail in Bulbeck *et al.* (1997). The method employs the temporal approximation in which periodic boundary conditions are imposed in both the streamwise and spanwise directions. Spatial discretisation involves using a Fourier Spectral method in the streamwise and spanwise directions and a fourth-order compact difference in the wall-normal direction with an algebraic mapping. The mapping parameter, y_o, determines the amount of stretching (large values give an equispaced grid). Temporal Discretisation is performed using a Crank-Nicholson implicit scheme for the wall-normal viscous terms, and third-order Runge-Kutta explicit for all other terms.

The initial condition for the simulation of the turbulent boundary layer was a restart file from the simulation of Spalart (1988), who performed a simulation at $Re_{\delta*} = 1000$ using a fully spectral numerical method. The velocity and vorticity fields from this restart file were interpolated using cubic-splines onto the algebraically-stretched grid and the interpolated values were used to start off the simulation. The grid used was $N_x \times N_y \times N_z = 128 \times 100 \times 192$ with $y_0 = 1.0$.

The simulation is run for $t = 6.25\delta/U_\infty$ non-dimensional time units, i.e. time enough to resolve about one and a half turbulence production/dissipation cycles in the buffer region. This corresponded to a total of 200 timesteps.

Statistics of time derivatives of the invariant quantities are computed at every second timestep, after the CFL number has been set to 0.015. This is done to minimise the error in the evaluation of the time

derivative. After the evaluation of the statistics of the dynamic quantities, the CFL number is reset to 0.25 for the next timestep.

INVARIANTS OF THE VELOCITY GRADIENT TENSOR

The local flow pattern (topology) at a given point in the flow field is determined by P, Q, and R, the invariants of the velocity gradient tensor $\mathbf{A}$ where the components of $\mathbf{A}$ are $A_{ij} = \partial u_i/\partial x_j$. The invariants, P, Q, and R are the coefficients which appear in the characteristic equation of $\mathbf{A}$ (Chong *et al.* (1990)). If the flow is incompressible then $P = 0$, $Q = -Tr[\mathbf{A}^2]/2$ and $R = -Tr[\mathbf{A}^3]/3$. The local flow pattern is determined by the location of the values of the (Q, R) pair on the Q-R plane. Figure 1. of Bulbeck *et al.* (1997) shows all possible local topologies in incompressible fluid flows. Invariants of the rate-of-strain tensor $S_{ij} = (A_{ij} + A_{ji})/2$, denoted by (Q_s, R_s) and the rate-of-rotation tensor $W_{ij} = (A_{ij} - A_{ji})/2$, denoted by (Q_w, R_w), are obtained in a similar fashion. In incompressible flow, $R_w = 0$. The discriminant D is given by $D = 27/4R^2 + Q^3$. The line $D = 0$ separates points with focal topology (positive D) from points with a node-saddle-saddle topology (negative D).

Invariants can also be used to derive equations for other quantities such as vortex stretching, σ, magnitude of the stretching vector, ε, dissipation of kinetic energy, ϵ and enstrophy, ω^2. These and some other important relations are

$$Q = Q_s + Q_w \quad (1)$$

$$R = R_s - W_{ki}S_{ij}W_{jk} = R_s - \Sigma \quad (2)$$

$$\sigma = \frac{\omega_i S_{ij} \omega_j}{\omega_k \omega_k} = \frac{\Sigma}{Q_w} \quad (3)$$

$$\epsilon = -4\nu Q_s \quad (4)$$

$$\omega^2 = 4Q_w \quad (5)$$

$$\varepsilon = V_i^{st} V_i^{st} \text{ where } V_i^{st} = S_{ij}\omega_j \quad (6)$$

Evolution of the Velocity Gradient Tensor

The evolution equation for A_{ij} is derived by differentiating the Navier-Stokes equations for the evolution of u_i by x_j. Equations for the evolution of the invariants of the velocity gradient tensor and related quantities Q and R are derived by manipulation of the evolution equation for A_{ij} and by using the Cayley-Hamilton theorem, yielding

$$\frac{dQ}{dt} = -3R - A_{mn}H_{nm} \quad (7)$$

$$\frac{dR}{dt} = \frac{2}{3}Q^2 - A_{mn}A_{nk}H_{km} \quad (8)$$

$$\frac{dR_s}{dt} = \frac{2}{3}Q_s Q + \frac{1}{4}\varepsilon - S_{ij}S_{jk}H_{ki} \quad (9)$$

$$\frac{dQ_s}{dt} = -2R_s - R - S_{ij}H_{ji}^S \quad (10)$$

$$\frac{d\varepsilon}{dt} = -\frac{16}{3}(R_s - R)Q + 2S_{ij}\omega_j(H_{il}^S\omega_l + S_{ik}\omega_k^H) \quad (11)$$

H_{ij} contains anisotropic pressure and viscous terms. Here H_{ij}^S refers to the symmetric part of the H_{ij}, and ω_i^H refers to the vector associated with the antisymmetric part of H_{ij} i.e. $\omega_i^H = \epsilon_{ijk}H_{kj}^W$, ϵ_{ijk} in this case being the alternating third-order tensor. The remaining two quantities Q_w and σ can be recovered from Eqns. 1, 2 and 3.

Models for H_{ij} have been proposed. The case for which $H_{ij} = 0$ is the Restricted Euler Model (REM)(Vieillefosse (1984), Cantwell (1992)). Dopazo *et al.* (1993) proposed the model, called the Linearised Diffusion Model (LDM), $H_{ij} = -\omega_o A_{ij}$ which gives the following equations for the evolution of the invariants and related quantities:

$$\frac{dQ}{dt} = -3R - 2\omega_o Q \quad (12)$$

$$\frac{dR}{dt} = \frac{2}{3}Q^2 - 3\omega_o R \quad (13)$$

$$\frac{dR_s}{dt} = \frac{2}{3}Q_s Q + \frac{1}{4}\varepsilon - 3\omega_o R_s \quad (14)$$

$$\frac{dQ_s}{dt} = -2R_s - R - 2\omega_o Q_s \quad (15)$$

$$\frac{d\varepsilon}{dt} = -\frac{16}{3}(R_s - R)Q - 4\omega_o\varepsilon \quad (16)$$

Here ω_o is an inverse diffusion timescale. The solution of the evolution equations using the LDM is an exponential decay of the discriminant

$$D(t) = D_o e^{-6\omega_o t} \quad (17)$$

Numerical Solution of the Evolution Equations

Equations 7 to 11 with $H_{ij} = 0$ (REM) and Equations 12 to 16 with $\omega_o = .2$ (LDM) are solved numerically using a fourth-order Runge-Kutta scheme. Eleven solution trajectories are computed from eleven different initial values of discriminant with $D_{min} = -4$, $D_{max} = 4$ and $\Delta D = .8$. The other initial conditions are: $R = -1$; $R_s = .5$; $Q_s = -4$; $\varepsilon = 10$. Solution trajectories are shown in Figures 1(a),(b), 2(a),(b) and 3(a),(b). Further details of the numerical solution can be found in Bulbeck (1998).

CONDITIONAL MEAN TRAJECTORIES

Conditional Mean Trajectories (CMTs) for the whole boundary layer are presented in Figures 1(c), 2(c) and 3(c). CMTs are the integral curves in probability space of the two-dimensional vector field comprising the conditional expected values (CEV) of the time derivatives of two quantities (Martin *et al.* (1997)).

The CMT of Q-R is presented in Figure 1(c). There is a periodic cycle of topology change from SF/S to UF/C, followed by a change in the sign of the discriminant to USN/S/S, then to SN/S/S, and finally back to SF/S. As the CMTs are computed from

the total time derivative, the spiralling of the CMTs are statistically representative of a cycle of topology change a particle in the flow will, on average, experience. The models of the evolution of Q and R present a somewhat different picture to the simulation data. The REM (Figure 1(a)) predicts no such spiralling motion; the discriminant must stay constant, and both R and Q become singular in finite time in this model. In the LDM (Figure 1(b)), trajectories moving toward the origin are permitted. However, the discriminant decays exponentially (Equation 17), and so no changes of sign of discriminant are permitted.

The Q_s-R_s CMTs are presented in Figure 2(c). These CMTs feature a critical point at the origin and another from which trajectories spiral outwards in a clockwise direction. This second critical point corresponds approximately to the location $(0.1, -1.2)$. Considering the CMTs as phaseplots in probability space, this critical point is an unstable focus, and the other critical point is a stable node at the origin. The peak mean Q_s from the DNS is estimated to be $\bar{Q}_s = -1.67$. This value of Q_s corresponds reasonably closely to the vertical location of the unstable focus in Figures 2(c). The trajectories of the solutions to the equations for the evolution of Q_s and R_s, presented in Figure 2(a) and (b) show qualitative similarity with the data. Those trajectories with initially positive discriminant will increase their value of $|Q_s|$ and eventually turn around and go towards the origin. The solution trajectories when the LDM is used show better agreement with the data when $R_s < 0$. The main discrepancy between the solution trajectories and the CMTs lies in the fact that the trajectories predicted by both models show no sign of spiralling around the critical point. The turbulent energy cascade is an inviscid process involving the generation of smaller and smaller scales of motion (corresponding to larger and larger values of $|Q_s|$) through nonlinear interactions. The CMTs for Q_s and R_s indicate that this process of generation of small scales of motion occurs in regions of the flow where the intermediate rate-of-strain is positive.

The CMTs of $-Q_s$-Q_w, presented in Figure 3(c), spiral clockwise around and in towards a stable focus at a critical point close to the mean values of $-Q_s$ and Q_w. The trajectories follow a path such that $-Q_s$ and Q_w both increase when $-Q_s > Q_w$, and decrease when $Q_w > -Q_s$. In this respect, the solution trajectories of the equations for the evolution of Q_s and Q_w using the LDM (see Figure 3(b)) and, to a lesser extent the REM (see Figure 3(a)), show a remarkably good agreement with the CMTs. They do not, however, show any spiralling motion about a critical point or a tendency to move towards regions along the Q_w axis, as the CMTs do. This region contains points with enstrophy and no dissipation, i.e. points performing solid-body rotation within vortex cores. The inability of the LDM to predict this tendency suggests that the effects of pressure gradients play an important role in driving particles into regions of positive discriminant, regions which are associated with the the cores of vortex structures.

CONCLUSION

Using DNS of a turbulent boundary layer, CMTs of invariant quantities have been computed and compared with solution trajectories of modelled equations for the evolution of the velocity gradient tensor. The clockwise spiralling of the trajectories in the Q-R, Q_s-R_s and Q_s-Q_w spaces was unable to be reproduced by the modelled equations. However, when the initial value of discriminant was zero or positive, the solutions to the modelled equations for the evolution of invariants were able to reproduce other features of the CMTs.

References

BULBECK, C. J. (1998). *An Investigation of the Invariants of the Velocity Gradient Tensor in Transitioning and Turbulent Boundary Layer Flow using Direct Numerical Simulation.* PhD thesis University of Melbourne.

BULBECK, C. J., CHONG, M. S., & SORIA, J. (1997). Investigating flow topologies in boundary layer transition using direct numerical simulation. *Appl. Sci. Research* **57**, 367–382.

CANTWELL, B. (1992). Exact solution of a restricted Euler equation for the velocity gradient tensor. *Phys. Fluids A* **4**, 782.

CHONG, M., PERRY, A., & CANTWELL, B. (1990). A general classification of three-dimensional flow fields. *Phys. Fluids A* **2**(5), 765–777.

DOPAZO, C., VALINO, L., & MARTÍN, J. (1993). Velocity gradients in turbulent flows; stochastic models. In *Ninth symposium on "Turbulent shear flow"* Kyoto, Japan.

MARTÍN, J. & DOPAZO, C. (1995). Velocity gradient invariant evolution from a linear diffusion model. In *Proceedings of the Twelfth Australasian Fluid Mechanics Conference* The University of Sydney, Australia.

MARTIN, J., OOI, A., SORIA, J., & CHONG, M. (1998). The dynamics of the velocity gradient tensor in isotropic turbulence. *Phys. Fluids A* accepted.

SPALART, P. (1988). Direct simulation of a turbulent boundary layer up to $R_\theta = 1410$. *J. Fluid Mech.* **187**, 61–98.

VIEILLEFOSSE, P. (1982). Local interaction between vorticity and shear in a perfect incompressible fluid. *J. Physique* **43**, 837–842.

VIEILLEFOSSE, P. (1984). Internal motion of a small element of fluid in an inviscid flow. *Physica* **125A**, 150–162.

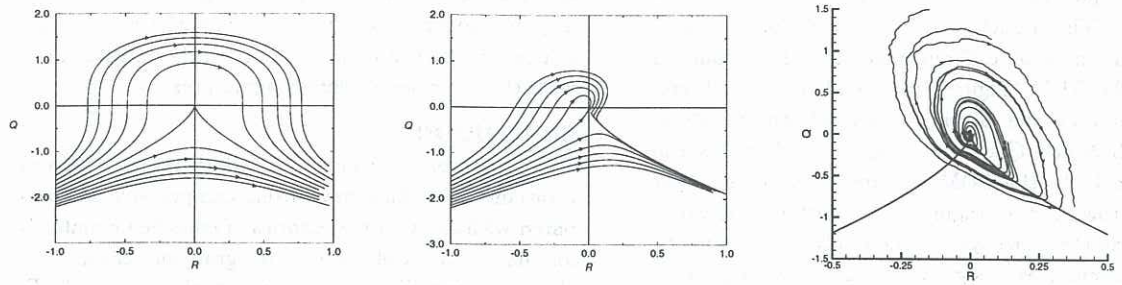

(a) (b) (c)

Figure 1: Q-R plane:(a) Restricted Euler Model. (b) Linearised Diffusion Model. (c) CMTs

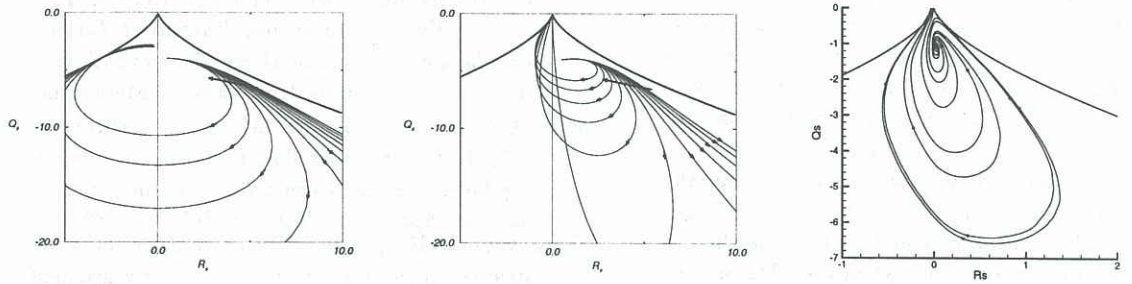

(a) (b) (c)

Figure 2: Q_s-R_s plane:(a) Restricted Euler Model. (b) Linearised Diffusion Model. (c) CMTs

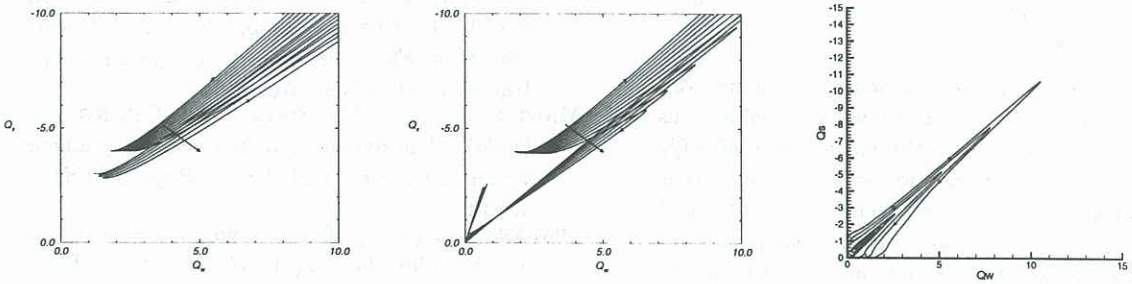

(a) (b) (c)

Figure 3: Q_s-Q_w plane:(a) Restricted Euler Model. (b) Linearised Diffusion Model. (c) CMTs